Degradation of biodegradable plastic films in soil: microplastic formation and soil microbial community dynamics

Yue Wang,[1] Run-Hao Bai,[1] Qi Liu,[1*] Qiu-Xiang Tang,[3] Chang-Hong Xie,[1] Aurore Richel,[4] Christophe Len,[5] Ji-Xiao Cui,[1,2] Chang-Rong Yan,[1] Wen-Qing He.[1,2*]

[1] Key Laboratory of Prevention and Control of Residual Pollution in Agricultural Film, Ministry of Agriculture and Rural Affairs, Institute of Environment and Sustainable Development in Agriculture, Chinese Academy of Agricultural Sciences, No. 12 Zhongguancun South Street, Beijing, 100081, China.

[2] Institute of Western Agricultural, Chinese Academy of Agricultural Sciences, No. 195 Ningbian East Road, Changji, 831100, China.

[3] Engineering Research Centre of Cotton, Ministry of Education/College of Agriculture, Xinjiang Agricultural University, No. 311 Nongda East Road, Urumqi, 830052, China.

[4] Laboratory of Biomass and Green Technologies, University of Liege, Gembloux 2 B-5030, Belgium.

[5] Chimie ParisTech, CNRS, PSL Research University, Institute of Chemistry for Life and Health Sciences, 11 rue Pierre et Marie Curie, Paris F-75005, France.

***Corresponding authors**

Wen-Qing He[*], E-mail: *hewenqing@caas.cn*, Phone and fax: +86-10-82109773.

Qi Liu[*], E-mail: *liuqi@caas.cn*, Phone and fax: +86-10-82105981.

Graphical abstract

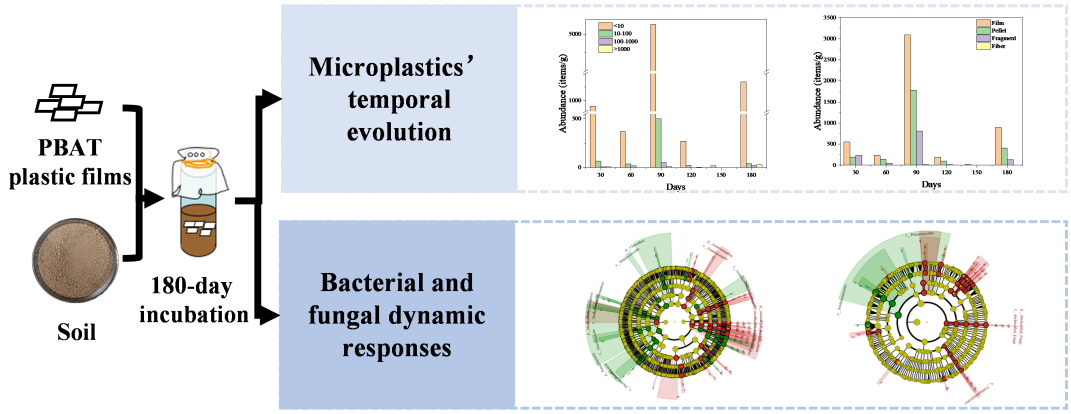

Highlights

- PBAT microplastics increase to peak and then decrease 74.7 % within 180 days.
- PBAT plastic films mainly release film-shape microplastics smaller than 10 μm.
- Revealed dynamic shifts in bacterial and fungal communities due to microplastics.
- Fungi prefer to release more PBAT microplastics by damaging PBAT's structure.
- Bacteria prefer to degrade PBAT microplastics by making them carbon sources.

Abstract

Biodegradable plastic poly(butylene adipate-co-terephthalate) (PBAT) has raised concerns about the release of PBAT microplastics and their potential environmental risks. In this study, PBAT plastic films were incubated in soil for 180 days to investigate the temporal evolution of PBAT microplastics and the dynamic responses of soil bacteria and fungi. The results showed that PBAT microplastics increase to peak and then decrease 74.7 % within 180 days. The dominant microplastics were smaller than 10 μm and in film shape. Based on the temporal patterns, three distinct phases were identified: the initial release period (0-30 days), the critical release period (60-120 days), and the critical degradation period (150-180 days). Notably, the dominant fungal biomarkers, particularly Humicola and Schizothecium, preferred to release more PBAT microplastics by damaging PBAT's structure, while the dominant bacterial biomarkers, such as Verrucomicrobiota, preferred to degrade PBAT microplastics by making them carbon sources. Our findings provide a new perspective

on systematically evaluating the environmental behavior and potential environmental risks of biodegradable microplastics and provides theoretical ideas for accelerating the degradation of biodegradable microplastics in soil environments.

Keywords

Poly (butylene adipate-co-terephthalate), Biodegradable microplastics, Microplastics formation, Microplastics degradation, Soil bacteria, Soil fungi

Environmental implication

This study involves the environmental risks of degradation of biodegradable plastic films, particularly PBAT films, in soil. In this study, PBAT microplastics, mainly with <10 μm size and film shapes, increased to peak and then decrease 74.7 % and affected the diversity, structure and composition of microbial communities during 180-day soil incubation. Dominant fungal and bacterial biomarkers respectively preferred to release and degrade PBAT microplastics. The dynamic responses of bacteria and fungi to PBAT microplastics indicated a shift in microbial function, suggesting that the release and degradation of biodegradable microplastics might alter the soil microenvironment and nutrient cycling over time.

1 Introduction

Polyethylene (PE), the most commonly used plastic in films and packaging, contributes significantly to residual plastic and microplastic pollution due to its widespread use and non-biodegradability [1–3]. Poly(butylene adipate-co-terephthalate) (PBAT) with favorable mechanical properties and biodegradability has been widely used and is expected to replace PE to reduce the residual plastic pollution [4–7]. Previous studies have shown that PBAT exhibits conditional degradability and releases PBAT microplastics in natural environments such as water, air and soil, as well as in aerobic and anaerobic composting conditions [8–13]. PBAT is found easy to release more microplastics compared with PE, which raises concerns about the potential environmental impact and safety risks of PBAT and hinders its promotion [9]. Soil environment is the main repository of microplastics, because microplastics in water and air transfer faster than in soil and

easy transfer to soil according to atmospheric fallout, runoff, groundwater migration, and hydrodynamics [14,15]. Therefore, it is necessary to investigate PBAT microplastics on its durability and degradability under soil environment, and its impact on soil microorganism.

PBAT microplastics have been found to show an abundance change of first increasing and then decreasing over time, and its abundance, size and shape are more prone to change than PE microplastics in previous laboratory and farmland experiments [16,17]. A laboratory incubation experiment with PBAT and PE microplastics found that the abundance of PBAT microplastics increased within 14 days and decreased to 21.9 % of the initial in 14 to 100 days, with decreased sizes and changed shapes. Under the same conditions, the abundance, sizes and shapes of PE microplastics were relatively stable [17]. The experiment above has analyzed the dynamics of the abundance, size and shape of PBAT and PE microplastics at 20 to 250 μm sizes artificially added in soil but ignore the process of microplastics released form plastic films, during which PBAT microplastics probably show more complex dynamics. In another research of PBAT based films mulching in farmland, the abundance of microplastics at 0.1 to 5 mm released from films into soil reached a peak of 350 to 525 item/kg after 2.5 years and decreased to 50 to 125 items/kg [16]. This farmland experiment has explored the abundance dynamics of microplastics released from plastic films, but the uncertain composition of microplastics and the complexity of field environments make the results unreliable. Building on the degradability of PBAT plastics, PE microplastics would remain with larger size for longer time in soil, while PBAT microplastics might be degraded into smaller size ones for shorter retention and used by soil microorganisms to reduce microplastics pollution [8,18]. To track the temporal evolution of PBAT microplastics during release and degradation, laboratory experiments with less environmental impacts are needed to explore the abundance and morphological characteristics PBAT microplastics with smaller sizes than previous. This is the meaningful premise to further explore the potential environmental risks of PBAT microplastics.

Soil microorganisms, key components of soil ecosystems, play an important role

in degrading PBAT and assessing the potential environmental risks of PBAT microplastics [19]. Previous studies have studied the effect of PBAT microplastics on soil microorganisms. PBAT microplastics has been found to promote carbon transferring into soil aggregates, significantly affecting soil conductivity, NO_3-N and TP contents, and pH, which potentially affect soil microorganisms by changing soil properties [18,20]. PBAT has been confirmed as persistent carbon resources to intensify competitive interactions of microbial food webs, increase the abundance of some microorganisms likes Aspergillus and Penicillium, and affect their roles in nutrient cycling and soil health [21–23]. PBAT microplastics can be colonized by soil microorganisms, creating a distinct microhabitat like the "plastisphere" in aquatic systems [24]. The abundance of PBAT microplastics influence soil bacterial diversity and richness, with effects that may vary depending on the shapes of microplastic likes those of PE microplastics [20,25]. Despite there are growing interest in PBAT microplastics under soil environment, current studies have not been able to fully reveal interactions between PBAT microplastics and soil microbes, especially microbes' potential capable of speeding up degradation of PBAT microplastics. In summary, further research is needed to understand the detailed interactions between PBAT microplastics and soil microorganisms, including the effects on bacterial and fungal diversity, community structure, and ecological functions, as well as the potential biodegradation of PBAT microplastics by soil microorganisms.

Under the above research background, we conducted a 180-day soil incubation of PBAT plastic films to study the temporal evolution of PBAT microplastics and the dynamic response of soil bacteria and fungi. The micromorphology, residual weight, mineralization, and molecular weight of PBAT were tested to elucidate the degradation characteristics of PBAT during incubation. PBAT microplastics were separated from soil through density separation method and measured by micro-Fourier-transform infrared spectroscopy (μFTIR) to analyze their temporal abundance and morphological characteristics. Important periods were identified based on the temporal evolution of PBAT microplastic. To figure out the dynamics of soil bacteria and fungi, the diversity, structure and composition of soil bacterial and fungal

communities were studies by amplicon sequencing, and their co-occurrence networks and predicted functions were further studies during different periods. This study can provide theoretical basis and technical support for systematically evaluating the environmental behavior and potential environmental risks of biodegradable microplastics, offering valuable insights for risk assessment and management strategies.

2 Materials and methods

2.1 Materials and soil

The polybutylene adipate-co-terephthalate (PBAT) used in this study was provided by Jinhui Zhaolong (Shanxi, China). PBAT was made into 30 μm thick PBAT film by extrusion blow moulding and was cut into 5 mm × 5 mm film slices for soil incubation experiments. The yellow–brown soil sample was collected from Shunyi District, Beijing, China (40°06′N, 116°55′E), and was sieved through a 2 mm mesh after air-drying. The soil contains a total organic carbon (TOC) content of 17.65 g/kg and a soil organic nitrogen (SON) content of 0.65 g/kg and has a pH value of 7.6. Before the PBAT soil-incubation experiment, a one-week soil incubation was setup to preserve soil microbial activity characteristics.

2.2 Experimental design

The PBAT soi-incubation experiments were carried out in 30-mL glass culture bottles with breathable films (BS-QM-01A, Biosharp, China). In experimental treatments (BP), we buried 100-mg PBAT slices in 10-g soil per bottle. To ensure full contact between PBAT and soil as much as possible, PBAT was positioned at the centre approximately 1 cm from both the soil surface and bottom. The control treatments (CK) consisted of soil without PBAT. The experimental and control treatments were set up with three replicates for each destructive sampling point. The incubation experiments were conducted over 180 days at a temperature of 25°C ± 1°C in darkness. Autoclaved Milli-Q water was added to maintain a soil water content of 20% during the incubation process. Gas samples were collected from headspace gases every five days to determine the mineralization rate of PBAT. The residual PBAT

samples and whole bottles soil samples were destructively collected every 30 days. The residual PBAT samples were cleansed and dried for the test of micromorphology, weight loss rate, and weight-average molecular weight of PBAT. The PBAT microplastics and microbial DNA were separated and extracted from soil samples, respectively.

2.3 Micromorphology observation

The surface micromorphology of PBAT film samples before and after incubation were observed by a scanning electron microscopy (SEM) (SU8010, Hitachi, Japan) operating at an acceleration voltage of 20 kV. Prior to SEM testing, samples were affixed to carbon conductive adhesive tape and then sputter-coated with a 10-nm layer of platinum/palladium alloy (80/20 w/w ratio) using a sputter coater (208HR, Cressington Scientific Instruments Ltd., Watford, England).

2.4 Weight loss rate test

The PBAT film samples before and after incubation were weighed by a balance (AUW120D, Shimadzu, Kyoto, Japan) to determine the gravimetric mass loss. The weight loss rate was obtained by calculating the percentage of gravimetric mass loss to the mass of PBAT film samples before incubation.

2.5 Mineralization rate test

Gas samples were collected from headspace gases using gastight syringes after bottles were sealed by stoppers featuring septa for 0 and 1 hour. The carbon dioxide (CO_2) concentrations of gas samples were tested by a gas chromatography (GC) instrument (HP4890D, Agilent, Wilmington, DE, USA) and was determined by referencing the calibration curve obtained using a calibration gas mixture with the declared composition. GC was equipped with Porapak Q (1.829 m length, 80/100 mesh) and 5A molecular sieve (1.829 m length, 60/80 mesh) packed columns connected in series along with a thermal conductivity detector. Nitrogen was served as the carrier gas at a flow rate of 30 mL min^{-1}, with the column temperature set at 55°C. The mineralization rate of PBAT was calculated by computing the ratio of the cumulative CO_2 amount of BP during incubation, with that of CK incubations subtracted, to the theoretical maximum CO_2 yield from PBAT complete oxidation.

2.6 Weight-average molecular weight test

The weight-average molecular weight (M_W) of PBAT film samples before and after incubation were determined by gel permeation chromatography (GPC) (LC20, Shimadzu, Japan) coupled with a differential refractive index detector (RID-20, Shimadzu, Kyoto, Japan). Each PBAT film sample was solubilized in chloroform and was centrifuged and filtered through a polytetrafluoroethylene (PTFE) filter to remove insoluble materials. 100-μL filtrate was injected into the analytical system at a flow rate of 1 mL/min. Tetrahydrofuran (THF) served as the solvent and was maintained at 40°C. Polystyrene (PS) standards were used for calibration.

2.7 Microplastics separation and analysis

Microplastics samples were separated from soil samples in each destructive sampling point through density separation method. Pretreated saturated NaI solution at a density of 1.75 g/cm^2 was served as the flotation agent for density separation. Each 3.7-g soil sample was mixed with the flotation agent in a tall beaker by a multi-joint magnetic stirrer (Kylin Bell, GL-6250, China) at stir rate 255 r/min. To break up soil aggregates and release more microplastics, the mixed solution underwent ultrasonic treatment at 20 kHz for 30 min before 12-h standing. After standing treatment, the clear upper solution was collected and transferred to another beaker. The flotation agent was added into the rest of the solution and then underwent the secondary mixing, ultrasonic, and standing treatment. The clear upper solution of the secondary treatment solution was mixed with the solution obtained previously and filtered using a 0.45-μm polytetrafluoroethylene (PTFE) membrane filter. We thoroughly rinsed the filter with 15% H_2O_2 and subjected the resulting solution to a 40 ℃ water bath for 24h to remove organic matter. The solution after water bath was filtered using a 0.2 μm Anodisc^{TM} 47 membrane filter (Cytiva, Whatman, Germany) to collect microplastics.

Microplastics retained on filters were analyzed by a μFTIR imaging microscope (Bruker Lumos II, Optik GmbH, Germany) in transmission mode in a wavenumber range between 1250 and 3600 cm^{-1} as described by Jakobs et al [26]. Backgrounds were measured on blank filters with the same settings. We use particles editor in

Bayreuth Microplastics Finder described by Hufnagl et al [27] to identify and quantify PBAT microplastics. To ensure the correct identification, we did double-check FTIR spectra of automatically classified microplastics. The shapes of PBAT microplastics were identified using length : width : height (L:W:H) ratios and Corey shape factor (CSF) distributions described by Merel Kooi et al [28].

2.8 DNA extraction and amplicon sequencing

DNA of soil samples in each destructive sampling point were extracted using TGuide S96 Magnetic Soil/Stool DNA Kit (Tiangen Biotech Co., Ltd. Beijing, China) according to manufacturer's instructions and kept at -40℃. There were triplicates peer samples. Bacterial amplicon libraries were generated by amplifying the full-length region of 16S rRNA using primers 27F (16S-F): 5'-AGRGTTTGATYNTGGCTCAG-3') and 1492R (16S-R): 5'-TASGGHTACCTTGTTASGACTT-3'. Full-length regions of fungal ITS regions were amplified using the primers ITS1F (5'-CTTGGTCATTTAGAGGAAGTAA-3') and ITS4 (5'-TCCTCCGCTTATTGATATGC-3').

BMKCloud (Biomarker, Beijing, China), based on PacBio sequencing platform, was used to perform sequence results. Single-molecule real-time sequencing (SMRT) Link software (version 8.0) with minPasses ≥ 5 and minPredictedAccuracy ≥ 0.9 was used to obtain circular consensus sequencing (CCS) reads. Version 1.7.0 of lima was employed to map CCS sequences to their respective samples via barcodes. Reads lacking primers and those exceeding the length criteria (1,200–1,650 bp) were eliminated through the identification of forward and reverse primers and via Cutadapt's quality control (version 2.7). The UCHIME algorithm (version 8.1) was utilized to identify and eliminate chimeric sequences, resulting in clean reads. USEARCH (version 10.0) clustered sequences with ≥97% similarity into operational taxonomic units (OTUs), with OTUs having an abundance of less than 0.005% being filtered out. Taxonomic classification of the OTUs was conducted using the naive Bayes classifier within QIIME2, employing the SILVA database (release 132) for bacterial 16S and the UNITE database (version unite.v7) for fungal ITS, with a 70%

confidence threshold.

2.9 Statistical analysis

PBAT degradation characteristics and results about PBAT microplastics were analyzed using Origin 2021. Operational taxonomic units (OTUs) of bacteria and fungi in BP and CK treatments were analyzed using R v3.1.1 (VennnDiagram-v1.6.9). Alpha diversity analysis of bacterial and fungal communities was performed using R v3.1.1 (picante, v1.8.2). Beta diversity analysis was performed using QIIME1.8.0 (principal_coordinates.py), employing principal coordinate analysis (PCoA) based on Binary–Jaccard distance for bacterial and fungal community analysis. The relative abundances of the top 10 phyla and top 20 genu of soil bacteria and fungi were calculated using python2 (matplotlib-v1.5.1) and R v3.1.1 (pheatmap, v1.02.), respectively. Linear discriminant analysis (LDA) effect size (LEfSe) was employed to test significant taxonomic differences among the groups and discover biomarkers from phylum to genus level using python 2 (Lefse). The LDA scores were greater than 3.0. The biotic co-occurrence networks of bacterial and fungal communities were analyzed using R-V3.6.1 (psych-v2.1.9, igraph-v1.2.5, visNetwork-v.2.1.0). Picrust2 (2.3.0) and FUNGuild (1.0) were used to predict functions of bacterial and fungal communities, respectively.

3 Results

3.1 Morphology and degradation characteristics of PBAT in soil

The morphology of the surface of PBAT during 180-day incubation is shown in Fig. 1a. With increasing incubation days, the microbial mycelium on the PBAT surface, as well as the breakage and roughness of PBAT, progressively increased. These observations suggest that soil microorganisms might degrade PBAT according to releasing enzymes, leading to the breakage of PBAT's molecular chain and the formation of PBAT microplastics. Fig. 1b illustrates the degradation characteristics of PBAT, including the weight loss rate, the mineralization rate, and the reduction rate of M_W of PBAT, with these indicators increasing over the course of incubation. Based on the above results, significant changes occurred in both morphology and molecular

structures of PBAT during 150-180 days. After 180 days, the weight loss rate, mineralization rate, and reduction rate of M_W of PBAT were 31.86%, 16.19%, and 27.37%, respectively. It is evident that PBAT has underwent degradation into CO_2 and experienced a change in its molecular structure. Furthermore, the discrepancy between the weight loss and mineralization rates of PBAT suggests that a portion of PBAT may be converted into microplastics but has not been degraded into CO_2.

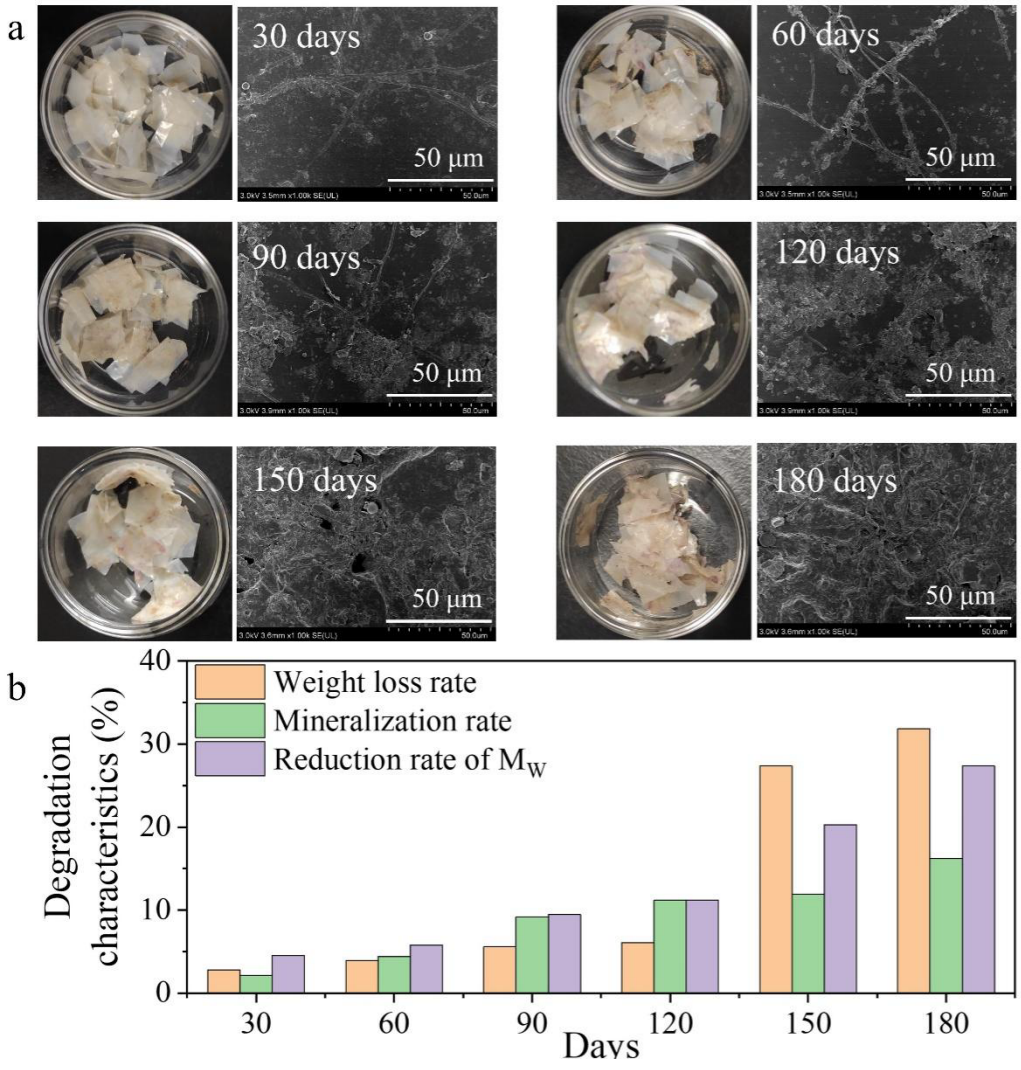

Fig. 1. Morphology and degradation characteristics of PBAT within 180 days of incubation in soil: (a) Pictures and scanning electron microscopy (SEM) images of residual PBAT samples isolated from soil; (b) The degradation characteristics of PBAT samples, including weight loss rate, mineralization rate, and reduction rate of weight-average molecular weight (M_W).

3.2 Release of PBAT microplastics during degradation

The abundances of PBAT microplastics generated from PBAT film degradation

are presented in Fig. 2a. The abundance of PBAT microplastics increased to 976 items/g after 30 days of incubation and further rose to 5695 items/g after 90 days. Subsequently, a decrease was observed, with the abundance of PBAT microplastics in range of 19 to 1438 items/g between 150 and 180 days. Based on the temporal evolution of PBAT microplastics, the periods of 0-30 days, 60-120 days, and 150-180 days are considered as the initial release period, the critical release period, and critical degradation period of PBAT microplastics, respectively. In comparison to the critical release period, PBAT microplastics experienced over 74.7 % degradation during the critical degradation period. Furthermore, we analyzed the relationships between the M_W of PBAT and its weight loss rate, mineralization rate and microplastics abundance using Allometricl, Logistic, and Bigaussian functions, as the variation in M_W is a key characteristic of PBAT degradation (Fig. 2b and Table S1). The results indicated that the weight loss rate and mineralization rate increased with M_W decreased. Additionally, significant release of PBAT microplastics were observed when $75000 < Mw < 80000$. The abundances of PBAT microplastics with different sizes and shapes during the 180-day incubation are presented in Fig. 2c and d. Images of PBAT microplastics in various shapes are shown in Fig. 2e. The classifications of PBAT microplastic by size and shape indicates that those with a size less than 10 μm or in film shape accounted for the majority of the total PBAT microplastics during the 180-day incubation. The temporal evolutions of PBAT microplastics with sizes less than 1000 μm, regardless of shapes, were consistent with that of total PBAT microplastics. PBAT microplastics larger than 1000 μm were primarily released after 180-day incubation.

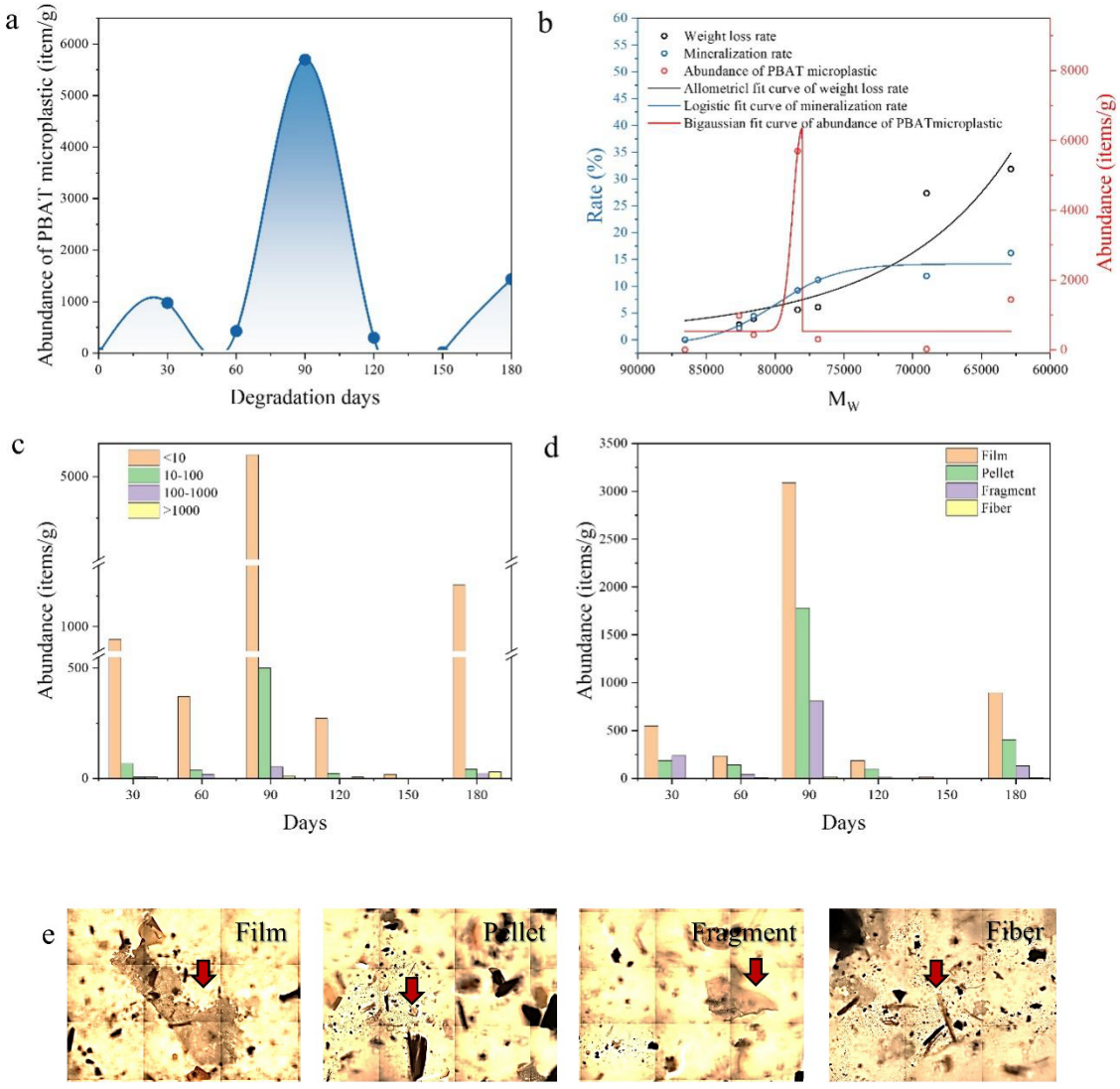

Fig. 2. The abundance of PBAT microplastics and its relationship with PBAT degradation characteristics: (a) The abundance of PBAT microplastics within 180 days of degradation; (b) The relationship between the abundance of PBAT microplastics and degradation characteristics of PBAT samples. The equations of fitted models are shown in Table S1; (c) The abundance of PBAT microplastics with different sizes within 180 days of degradation; (d) The abundance of PBAT microplastics with different shapes within 180 days of degradation; (e) Images of different shapes microplastics taken by Lumus II FTIR spectrometer.

Fig. 3 compares the abundances and temporal evolutions of differently shaped microplastics in PBAT microplastics, categorized by size: smaller than 10 μm, between 10-100 μm, between 100-1000 μm, and larger than 1000 μm. PBAT microplastics smaller than 10 μm predominantly exhibited a film shape (Fig. 3a). PBAT microplastics with size between 10-100 μm were mainly represented by

fragment and pellet shapes during the initial release period and the critical release period, respectively (Fig. 3b). PBAT microplastics in fragment shape constituted the majority of those sized between 100-1000 μm, as well as those larger than 1000 μm (Figs. 3c and d).

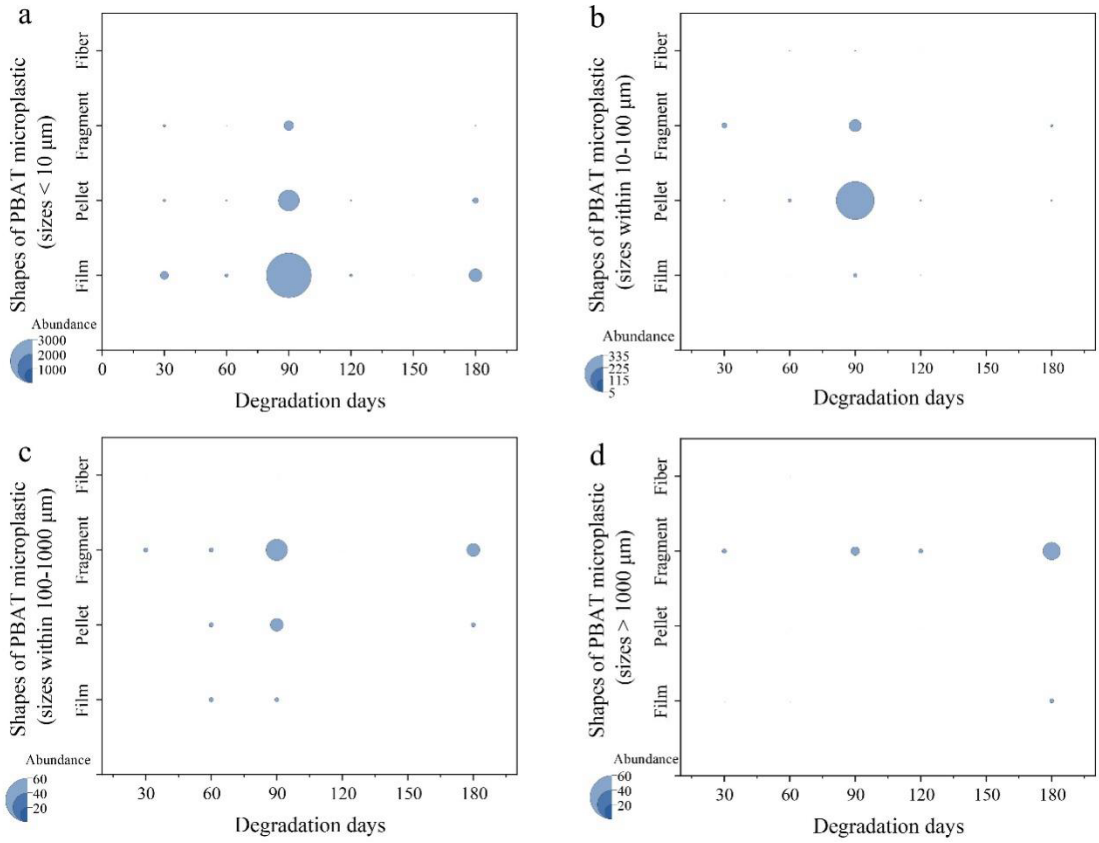

Fig. 3. The abundance of PBAT microplastics with different sizes and shapes within 180 days of degradation: (a) The abundance of different shaped PBAT microplastics with sizes below 10 μm; (b) The abundance of different shaped PBAT microplastics with sizes between 10 and 100 μm; (c) The abundance of different shaped PBAT microplastics with sizes between 100 and 1000 μm; (d) The abundance of different shaped PBAT microplastics with sizes upon 1000 μm.

3.3 Effects of PBAT microplastics on soil bacterial and fungal communities

3.3.1 The diversity, structure and composition of soil bacterial communities

The number of endemic and shared operational taxonomic units (OTUs) of bacterial communities in the BP and CK treatments were shown in Fig. 4a to display the similarity and overlap of the OTU composition of samples. The results of Alpha diversity (Figs. S1) reflect that PBAT microplastics have no significant effect on the richness and diversity of bacterial communities. However, a lower PBAT

microplastics abundance may lead to more bacterial endemic OTUs, while a higher one was the opposite (Fig. 4a). As the results of Principal Coordinate Analysis (PCoA) presented in Fig. 4d, incubation days exert a more significant influence on the composition of the bacterial community than the presence of PBAT microplastics. The detailed descriptions of these results are shown in Supplementary Materials (Text S1).

A total of 10 dominant phyla and 20 dominant genera were compared in both treatments in Fig. 4b and c to analyze the structure of soil bacterial communities. The detailed results are presented in Supplementary Materials (Text S1). PBAT microplastics may promote the survival of 3 phyla: *Verrucomicrobiota*, *Patescibacteria* and *Planctomycetota* and 3 genera: unclassified_Pedosphaeraceae, uncultured_soil_bacterium and uncultured_Microgenomates_group_bacterium, while negatively affecting 4 phyla: *Chloroflexi*, *Bdellovibrionota*, *Acidobacteritoa*, and *Nitrospirota* and 5 genera: *unclassified_Gemmatimonadaceae*, *unclassified_Vicinamibacterale*, *MND1*, *Nitrospira* and *unclassified_Vicinamibacteraceae*. PBAT plastics with small abundance provide more survival resources for *Candidatus_Omnitrophus*，*Flavisolibacter*，and *Massilia*, while those with large abundance are unconducive to their survival. The other bacterial genera might be initially sensitive to PBAT microplastics but could gradually adapt to such environments.

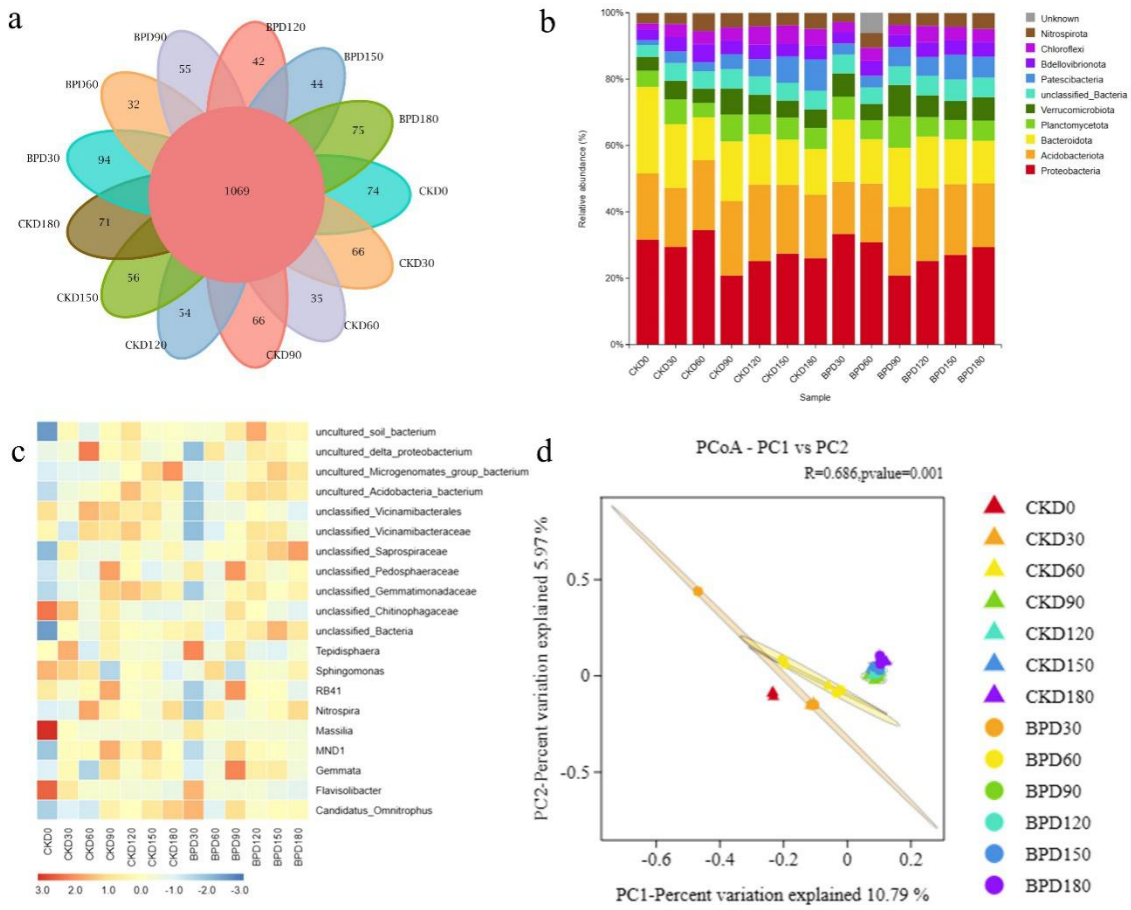

Fig. 4. Soil bacterial community composition and diversity analysis of BP and CK treatments in 0 day (D0), 30 days (D30), 60 days (D60), 90 days (D90), 120 days (D120), 150 days (D150), and 180 days (D180): (a) Veen diagram of OTU distribution to show different and shared OTU numbers between BP and CK treatments; (b) Relative abundance of the top 10 bacterial phyla; (c) Hierarchically clustered heatmap of the top 20 abundant bacterial genera; (d) Principal Coordinate Analysis (PCoA) of bacterial abundance.

3.3.2 The diversity, structure and composition of soil fungal communities

Figs. 5a and S2 show the numbers of endemic and shared OTUs and Alpha diversity indexes of fungal communities in BP and CK treatments, respectively. Fig. 5d depicts the differences and similarities in the composition of fungal communities between BP and CK treatments as revealed by PCoA. Supplementary Materials (Text S2) shows the detailed results of Figs. 5 and S2. The degradation and release of PBAT microplastics are associated with an increase and a decrease in the number of endemic fungal OTUs, respectively (Fig. S5a). Additionally, PBAT microplastics significantly enhanced the richness and diversity of fungal communities at 150 days (Fig. S2) and

significantly affect the composition of the fungal community during the critical release and degradation periods of PBAT microplastics (Fig. 5d).

Figs. 5b and c compare the relative abundances of 10 dominant fungal phyla and 20 dominant fungal genera between BP and CK treatments, respectively. Detailed descriptions about the results are presented in Supplementary Materials (Text S2). As shown in Fig. 5b, PBAT microplastics may favor the survival of dominant *Ascomycota* phyla, promote the survival of *Mucoromycota* at low abundances, but adversely affect its survival at high abundance. The remaining dominant 8 fungal phyla displayed initial sensibility to the presence of PBAT microplastics but gradually adapted to such environments. In Fig. 5c, PBAT microplastics may enhance the survival of 5 dominant fungal genera (*Schizothecium, Acrophialophora, Alternaria, Humicola, and Oidiodendron*), but might adversely impact the survival of *Fusarium*. Additionally, PBAT microplastics promote the proliferation of 4 fungal genera (*Chaetomium, Spizellomyces, Neonectria*, and *Aspergillus*) at low abundances, but detrimental effects at high abundance. The remaining 10 fungal genera showed initial sensibility to the presence of PBAT microplastics but gradually adapted to such environments.

In summary, during the 180-day evolution, PBAT microplastics have no significant effect on the diversity of bacterial communities but affect their composition and structure. In contrast, PBAT microplastics significantly affect the diversity, composition, and structure of fungal communities.

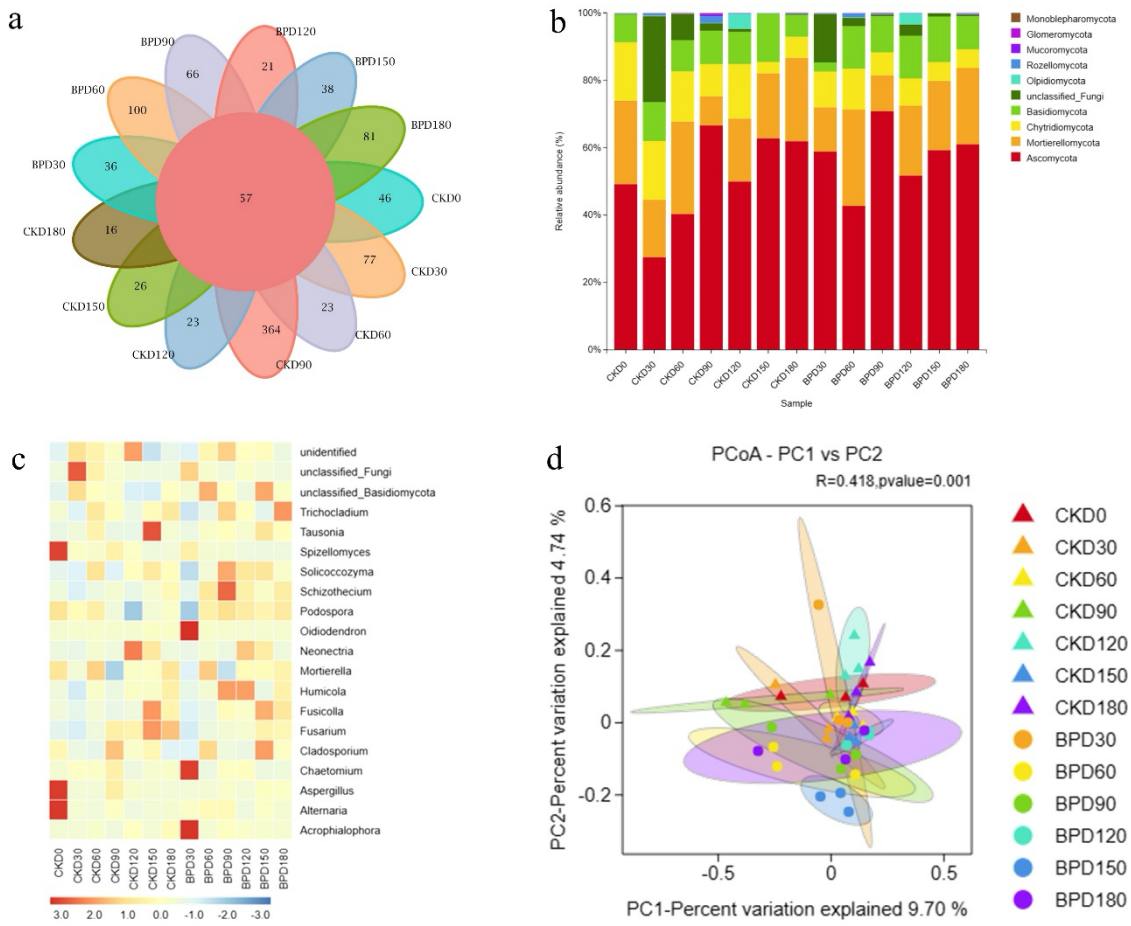

Fig. 5. Soil fungal community composition and diversity analysis of BP and CK treatments in 0 day (D0), 30 days (D30), 60 days (D60), 90 days (D90), 120 days (D120), 150 days (D150), and 180 days (D180): (a) Veen diagram of OTU distribution to show different and shared OTU numbers between BP and CK treatments; (b) Relative abundance of the top 10 fungal phyla; (c) Hierarchically clustered heatmap of the top 20 abundant fungal genera; (d) Principal Coordinate Analysis (PCoA) of fungal abundance.

3.4 Bacterial and fungal biomarkers at different periods

To identify bacterial and fungal biomarkers influenced by PBAT microplastics, we analyzed microbial relative abundance differences between BP and CK treatments. This analysis was conducted during three key periods: the initial release (0-30 days), critical release (60-120 days), and critical degradation (150-180 days) of PBAT microplastics, using Linear discriminant analysis effect size (LEfSe) (Fig. 6). The numbers of bacterial and fungal biomarkers in the three periods were critical degradation period, the critical release period, and the initial release period in order

from high to low. Detailed information about these biomarkers is shown in Supplementary Materials (Text S3). Among these biomarkers, Chaetomium was not only a fungal biomarker in BP treatments during the initial release period, but also a dominant fungal genus. The bacterial biomarker RB41 in CK treatments during the same period was a dominant bacterial genus. During the critical release period, 2 bacterial biomarkers (*Humicola* and *Schizothecium*) were dominant in BP treatments, while in CK treatments, 3 bacterial biomarkers (*Acidobacteriota* phylum, *unclassified_Vicinamibacteraceae* genus, and *unclassified_Vicinamibacterales* genus) were dominant. During the critical degradation period, 8 biomarkers were dominant in BP treatments, including 6 bacteria (*Verrucomicrobiota* and *unclassified_Bacteria* phyla, and *unclassified_Pedosphaeracea*e, *unclassified_Bacteria*, *unclassified_Saprospiraceae*, *uncultured_soil_bacterium* genera) and 2 fungi (*unclassified_Fungi* phylum and *unclassified_Fungi* genus). Additionally, there were 4 bacteria (*Chloroflexi* and *Patescibacteria* phyla, and *Candidatus_Omnitrophus* and *unclassified_Vicinamibacterales* genera) and 2 fungi (*Fusarium* and *Chaetomium* genera) were dominant biomarkers in CK treatments during this period. These 20 dominant biomarkers are probably related to the release and degradation of PBAT microplastics.

Fig. 6. The bacterial and fungal biomarkers of BP and CK treatments at 0-30 days, 60-120 days, and 150-180 days: (a-c) The bacterial biomarkers at 0-30 days, 60-120 days and 150-180 days; (d-f) The fungal biomarkers at 0-30 days, 60-120 days and 150-180 days.

3.5 Bacterial and fungal co-occurrence networks analysis and functions

prediction at different periods

To understand the dynamics of bacterial and fungal communities, we analyzed the topological properties of their co-occurrence networks (Figs. 7 and 8, Tables S2 and S3) and the proportion of predicted functional genes (Fig. 9) in BP and CK treatments during the initial release, critical release, and critical degradation periods of PBAT microplastics. The detailed results of bacterial and fungal co-occurrence networks analysis and functions prediction at different periods are shown in Supplementary Materials (Texts S4 and S5). During the initial release period, low-abundance PBAT microplastics likely enhance biodiversity by creating new habitats. This reduces the dependence of bacterial and fungal communities on specific microbial interactions, fostering ecological specialization and community diversification. There were more frequent interactions among fungi, while bacteria show the opposite trend. PBAT microplastics did not affect the functional genes of bacterial and fungal community during this period. During the critical release period, high abundance of PBAT microplastics enhanced the complexity and stability of these communities but reduced biodiversity and closeness and has stronger influence on the structure and functions of fungal community than on those of bacterial functions. Fungal community shows stronger degradation function and weaker disease function under the effect of high-abundance PBAT microplastics. During the critical degradation period, there were enhanced and more complex bacterial and fungal community functions, increased bacterial biodiversity but reduced bacterial complexity. In contrast, fungal communities displayed tighter structures with less reliance on specific communities. Bacterial communities show stronger potential degradation and utilization functions on PBAT microplastics during this period.

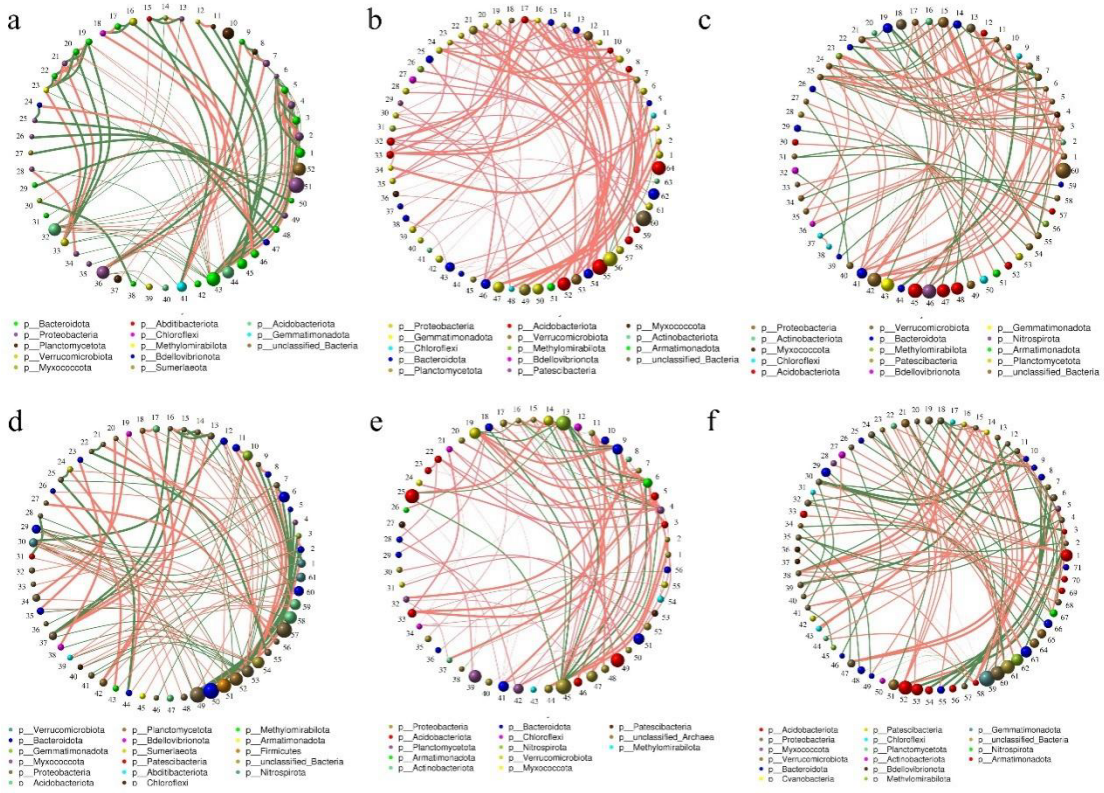

Fig. 7. Bacterial co-occurrence networks of BP and CK treatments at 0-30 days, 60-120 days, and 150-180 days: (a-c) Bacterial co-occurrence networks of CK treatments at 0-30 days, 60-120 days, and 150-180 days; (d-f) Bacterial co-occurrence networks of BP treatments at 0-30 days, 60-120 days, and 150-180 days.

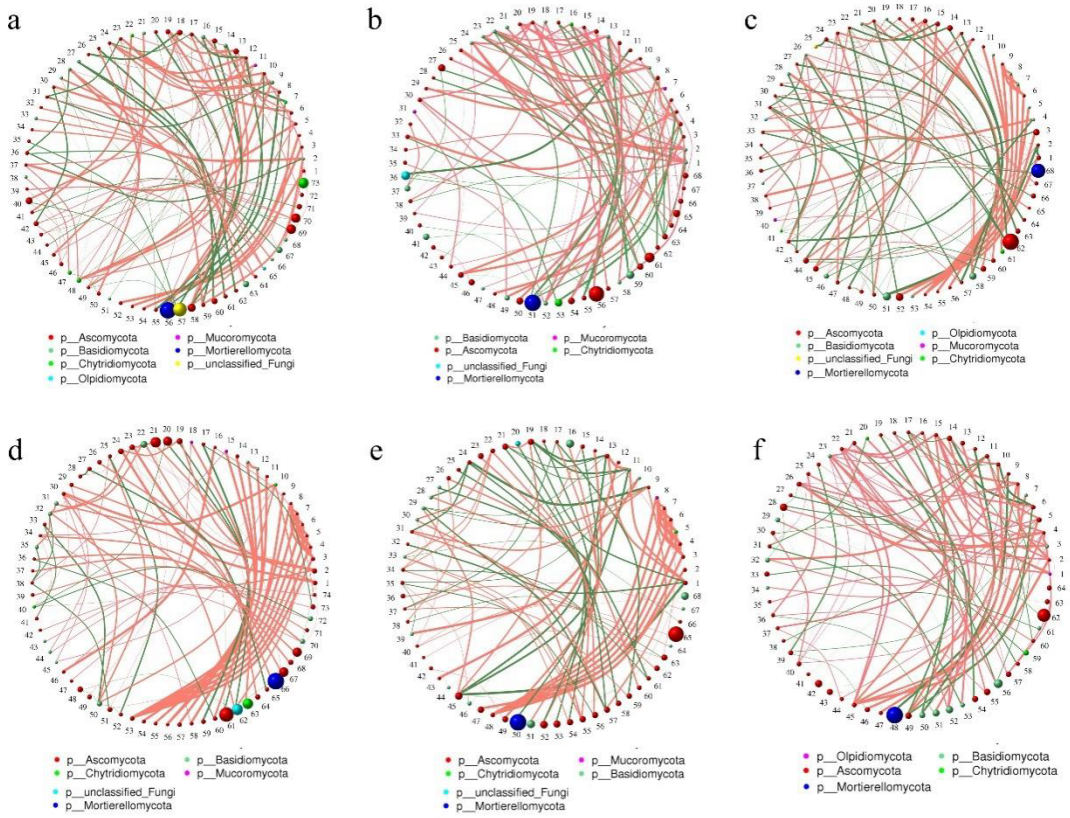

Fig. 8. Fungal co-occurrence networks of BP and CK treatments at 0-30 days, 60-120 days, and 150-180 days: (a-c) Fungal co-occurrence networks of CK treatments at 0-30 days, 60-120 days, and 150-180 days; (d-f) Fungal co-occurrence networks of BP treatments at 0-30 days, 60-120 days, and 150-180 days.

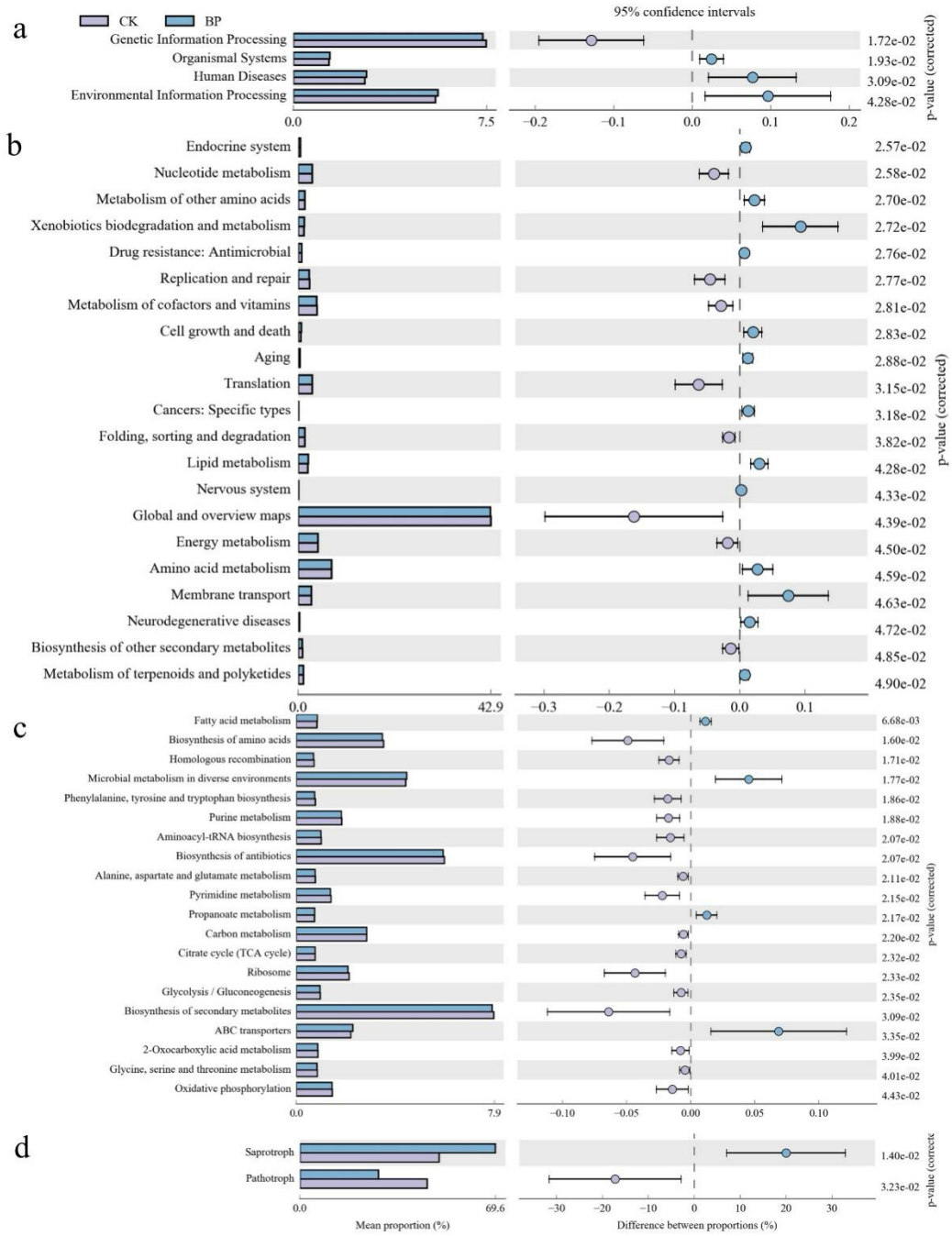

Fig. 9 The proportion of predicted bacterial functional genes among CK and BP treatments at different periods: (a-c) The proportion of predicted bacterial level-1, level-2, and level-3 functional genes at key period of PBAT microplastics degradation; (d) The proportion of predicted fungal trophic functional genes at key period of PBAT microplastics release.

4 Discussion

4.1 The temporal evolution of microplastics formed by PBAT plastic films in soil environment

During the 180-day incubation in soil, PBAT plastic films underwent microbial colonization and mineralization, leading to residual weight and molecule weight loss, and release of PBAT microplastics. Based on the temporal abundance of PBAT microplastics, the periods of 0-30 days, 60-120 days, and 150-180 days were respectively considered as the initial release period, the critical release period, and the critical degradation period of PBAT microplastics. The temporal abundance of PBAT microplastics first increased to peak and then decreased about 74.7 %. In addition, PBAT with 75000 < Mw < 80000 is prone to microplastic release, rapid weight loss and mineralization. These results indicate that the temporal abundance of PBAT microplastics formed by PBAT plastic films under soil environment was consistent with results of previous research adding PBAT microplastics into soil artificially [16,17]. Combined with previous research, our study confirms that PBAT microplastics must be fragmented to release more ones and then degraded leading to less ones under soil environment, regardless of whether intimal ones come from artificial additions or plastic films' formation.

This study conducted a detailed analysis of the sizes and shapes of PBAT microplastics, and the results showed that the dominant PBAT microplstics were at <10 μm size and film shape. Most previous studies were limited to detecting plastic particles > 20 μm with unclear shapes [16,17], we used better and more sophisticated analytical techniques [26–28] to detect and quantify them at different sizes and shapes. Our study provides more detailed evidence of the morphological characteristics of PBAT microplastics formed by PBAT plastic films in soil environment.

4.2 The dynamic responses of soil bacterial and fungal communities

During the temporal evolution of PBAT microplastices, PBAT microplastics have no significant effect on the diversity of bacterial communities but affect their composition about OTUs and their structure about dominant phyla and genera. For fungal communities, PBAT microplastics significantly affect their diversity, composition, and structure. It is worth noting that PBAT microplastics affect bacterial and fungal communities' composition in influencing the relative abundance of dominate phyla and genera and making 20 of them biomarkers of different period.

During the initial release period, low-abundance PBAT microplastics enhanced the biodiversity and specialization bacterial and fungal community by providing habitats. Bacteria and fungi reduced dependence on specific communities, with fungi interacting more frequently than bacteria. PBAT microplastics at low abundance favor the survival of *Chaetomium* but sensitize *RB41*. *Chaetomium* was reported to show PVC degradation potential and might be a putative plastic-degrader [29,30]. It may contribute to the initial release of PBAT microplastics by breaking down the PBAT polymer structure. *RB41* was one of main bacteria with carbon flux function [31], and the inhibition of it during this period might cause PBAT to prefer to release microplastics than mineralized. There might be functional differences between bacteria and fungi during this period, with the former possibly related to carbon source use and the latter possibly related to PBAT degradation.

During the critical release period, PBAT microplastics with high abundance increased bacterial and fungal community complexity and stability but decreased biodiversity and closeness. Fungal communities were more impacted structurally and functionally than bacterial ones, showing enhanced degradation and reduced disease functions. PBAT microplastics at high abundance favor the survival of *Humicola* and *Schizothecium* but negatively affect the survival of *Acidobacteriota, unclassified_Vicinamibacteraceae,* and *unclassified_Vicinamibacterales. Humicola* has been studied to produce cutinase with the function of degrading PBAT in previous studies [32–34]. *Schizothecium* was one of the dominant genera that might be associated with organic matter degradation or pollutant transformation [35]. These two fungi probably caused the enhanced degradation function of fungal communities during this period, which aggravates the damage of PBAT structure to release high abundance microplastics. The abundance of *Acidobacteriota* was found to be decreased by PE microplastics, biodegradable microplastics (PHA and PLA) and similar in our study [21,36]. There was no study to find the relationship between microplastics and *unclassified_Vicinamibacteraceae,* and *unclassified_Vicinamibacterales,* and they might be also sensitive to high abundance PBAT microplastics.

During the critical degradation period, bacterial and fungal community functions become more complex. Bacterial biodiversity increases but complexity decreases, likely due to PBAT degradation providing extra carbon sources. Fungal communities have tighter structures. Bacteria may have stronger degradation and utilization functions on PBAT microplastics. During this period, PBAT microplastics provide the survival of 8 biomarkers due to the low abundance or becoming the carbon sources, including bacterial *Verrucomicrobiota, unclassified_Bacteria* phyla, *unclassified_Pedosphaeraceae*，*unclassified_Bacteria*，*unclassified_Saprospiraceae*，*uncultured_soil_bacterium* genera, and *fungal unclassified_Fungi* phylum and *unclassified_Fungi* genus. *Verrucomicrobiota* was found carrying genes capable of degrading stable polysaccharides and its abundance increased under the effect of PBAT/PLA mulching film in previous studies [37–39], which makes PBAT easier to be degraded into carbon source by *Verrucomicrobiota*. The other 7 dominate biomarkers have no be studied, but we could make the similar guesses. At the same time, the survival of 6 biomarkers were conflicted, including bacterial *Chloroflexi, Patescibacteria* phyla, *Candidatus_Omnitrophus*, and *unclassified_Vicinamibacterales* genera, and fungal *Fusarium* and *Chaetomium* genera. *Chloroflexi* was found to play potential roles in sediment carbon cycling and carbon sequestering [40], so its decreasing survival in our study might be due to that PBAT prefers to be mineralized than be sequestered during this period. *Patescibacteria* was the main bacteria survival in the existence of PE, PP and PS microplastics and contributed toward break down of esters in previous studies [41,42] but decreased during this period in our study. *Fusarium* producing cutinase and *Chaetomium* were also found to be putative plastic-degraders in previous studies [29,30,43] but also decrease in our study. We hypothesize that the biodegradation process of PBAT microplastics during this period is mainly carried by microorganisms using carbon sources and mineralization, while there are less action sites for these 3 ones mainly damaging PBAT structure. The roles of *Candidatus_Omnitrophus*, and *unclassified_Vicinamibacterales* in microplastics and carbon transformation have not been studied previously, which is worth studying in future.

The discussion of the above 20 dominant biomarkers identified at different periods highlight their key roles on the dynamic responses of bacteria and fungi during the evolution of PBAT microplastics in the soil. During the initial release period, *Chaetomium* focused on damaging PBAT structures to release microplastics with low abundance to provide habitats and enhance the biodiversity and specialization bacteria and fungi. At the same time, PBAT preferred to release microplastics than mineralized so the carbon flux function of *RB41* is inhibited. Next, fungal communities enhanced the potential PBAT-degradation function during the critical release period and focused on releasing degrading enzymes mainly from *Humicola* and *Schizothecium* to aggravate the damage of PBAT structure and cause the high abundance of PBAT microplastics in soil. This inhibited the survival of *Acidobacteriota, unclassified_Vicinamibacteraceae,* and *unclassified_Vicinamibacterales* sensitive to microplastics. During the critical degradation period, bacterial communities were preferring to show stronger potential PBAT-degradation function and use PBAT as the carbon source. *Verrucomicrobiota* and another 6 dominant biomarkers made PBAT microplastics easier to be degraded into carbon source and decreased the abundance of PBAT microplastics. This process caused the decreasing sites in damaging PBAT structure functions of *Patescibacteria*, *Fusarium*, and *Chaetomium*. In addition, PBAT preferred to be mineralized than sequestered during this period, causing the decrease of *Chloroflexi* with carbon sequestering function. The roles of *Candidatus_Omnitrophus* and *unclassified_Vicinamibacterales* in microplastic evolution remain unclear and should be explored in future studies, as their potential involvement in PBAT degradation could provide more valuable insights into microplastic degradation mechanisms. Besides, this study mainly explores the roles of microorganisms playing in the degradation of PBAT microplastics. There is a direction worthy to research in the future about the metabolic pathways of microorganisms through genomics or metabolomics, and the mechanisms by which these pathways affect the rate of PBAT microplastics' degradation.

5 Conclusion

According to the 180-day soil incubation experiment PBAT plastic films, we studied the formation process of PBAT microplastics release and degradation in soil environment and dynamic responses of bacteria and fungi. There were 3 key periods PBAT microplastics underwent in soil: the initial release period, the critical release period, and the critical degradation period. The abundance of PBAT microplastics increased during the initial release period and increased to peak during the critical release period of about 90 days, then significantly decreased during the critical degradation period with a decrease of 74.7 % at 180 days. This indicates that PBAT would residual less microplastics in soil, or even complete disappearance. During this process, the response of soil microbial communities showed periodic dynamics, with significant effects on the composition and structure of bacterial communities and stronger diversity and degradation functions of fungal communities. Fungi such as *Humicola* and *Schizothecium* promoted the degradation of PBAT by enzymatic hydrolysis during the critical release period, while bacteria including *Verrucomicrobiota* accelerated the carbon conversion of PBAT through mineralization. Additionally, the degradation process of PBAT microplastics was accompanied by the influence of microbial communities on the transformation and selection of carbon sources. This study provides new insights into the microbial mechanisms of biodegradable plastics' degradation in soil and provides important basis for the development of microplastic pollution control strategies.

CRediT authorship contribution statement

Declaration of Competing Interest

Acknowledgements

This work was supported by Key Research and Development Task Project of Xinjiang Uygur Autonomous Region [grant numbers 2022B02033], National Natural Science Foundation of China [grant numbers 42007312, 32301967, 42211530566], "Project for Young Top-notch Talents-Young Scientific and Technological Innovation Talents" of the "Tianshan Talents" Training Program in Xinjiang [grant

numbers 2023TSYCCX0019], Inner Mongolia Autonomous Region Science and Technology Project [grant numbers 2022YFHH0042], International Exchanges 2022 Cost Share (NSFC) [grant numbers EC\NSFC\223123].

References

[1] L. Chen, Z. Lin, Polyethylene: Properties, Production and Applications, in: 2021 3rd Int. Acad. Exch. Conf. Sci. Technol. Innov., 2021: pp. 1191–1196. https://doi.org/10.1109/IAECST54258.2021.9695646.

[2] R. Qi, D.L. Jones, Z. Li, Q. Liu, C. Yan, Behavior of microplastics and plastic film residues in the soil environment: A critical review, Sci. Total Environ. 703 (2020) 134722. https://doi.org/https://doi.org/10.1016/j.scitotenv.2019.134722.

[3] M. MacLeod, H.P.H. Arp, M.B. Tekman, A. Jahnke, The global threat from plastic pollution, Science . 373 (2021) 61–65. https://doi.org/10.1126/science.abg5433.

[4] T. Burford, W. Rieg, S. Madbouly, Biodegradable poly(butylene adipate-co-terephthalate) (PBAT), Phys. Sci. Rev. 8 (2023) 1127–1156. https://doi.org/doi:10.1515/psr-2020-0078.

[5] H. Somanathan, R. Sathasivam, S. Sivaram, S. Mariappan Kumaresan, M.S. Muthuraman, S.U. Park, An update on polyethylene and biodegradable plastic mulch films and their impact on the environment, Chemosphere. 307 (2022) 135839. https://doi.org/https://doi.org/10.1016/j.chemosphere.2022.135839.

[6] H. Serrano-Ruiz, L. Martin-Closas, A.M. Pelacho, Biodegradable plastic mulches: Impact on the agricultural biotic environment, Sci. Total Environ. 750 (2021) 141228. https://doi.org/https://doi.org/10.1016/j.scitotenv.2020.141228.

[7] T.P. Haider, C. Völker, J. Kramm, K. Landfester, F.R. Wurm, Plastics of the Future? The Impact of Biodegradable Polymers on the Environment and on Society, Angew. Chemie Int. Ed. 58 (2019) 50–62. https://doi.org/https://doi.org/10.1002/anie.201805766.

[8] J. Liao, Q. Chen, Biodegradable plastics in the air and soil environment: Low degradation rate and high microplastics formation, J. Hazard. Mater. 418 (2021) 126329. https://doi.org/https://doi.org/10.1016/j.jhazmat.2021.126329.

[9] X.-F. Wei, M. Bohlén, C. Lindblad, M. Hedenqvist, A. Hakonen, Microplastics generated from a biodegradable plastic in freshwater and seawater, Water Res. 198 (2021) 117123. https://doi.org/https://doi.org/10.1016/j.watres.2021.117123.

[10] F. Convertino, S.C. Carroccio, M.C. Cocca, S. Dattilo, A.C. Dell'Acqua, L. Gargiulo, L. Nizzetto, P.M. Riccobene, E. Schettini, G. Vox, D. Zannini, P. Cerruti, The fate of post-use biodegradable PBAT-based mulch films buried in agricultural soil, Sci. Total Environ. 948 (2024) 174697. https://doi.org/https://doi.org/10.1016/j.scitotenv.2024.174697.

[11] A. Mercier, K. Gravouil, W. Aucher, S. Brosset-Vincent, L. Kadri, J. Colas, D. Bouchon, T. Ferreira, Fate of Eight Different Polymers under Uncontrolled Composting Conditions: Relationships Between Deterioration, Biofilm Formation, and the Material Surface Properties, Environ. Sci. \& Technol. 51 (2017) 1988–1997. https://doi.org/10.1021/acs.est.6b03530.

[12] Y. Jin, F. Cai, C. Song, G. Liu, C. Chen, Degradation of biodegradable plastics by anaerobic digestion: Morphological, micro-structural changes and microbial community dynamics, Sci. Total Environ. 834 (2022) 155167. https://doi.org/https://doi.org/10.1016/j.scitotenv.2022.155167.

[13] Y. Ren, J. Hu, M. Yang, Y. Weng, Biodegradation Behavior of Poly (Lactic Acid) (PLA), Poly (Butylene Adipate-Co-Terephthalate) (PBAT), and Their Blends Under Digested Sludge Conditions, J. Polym. Environ. 27 (2019) 2784–2792. https://doi.org/10.1007/s10924-019-01563-3.

[14] Q. Zhou, J. Zhang, M. Zhang, X. Wang, D. Zhang, X. Pan, Persistent versus transient, and conventional plastic versus biodegradable plastic? —Two key questions about microplastic-water exchange of antibiotic resistance genes, Water Res. 222 (2022) 118899. https://doi.org/https://doi.org/10.1016/j.watres.2022.118899.

[15] M.B. Alfonso, A.H. Arias, A.C. Ronda, M.C. Piccolo, Continental microplastics: Presence, features, and environmental transport pathways, Sci. Total Environ. 799 (2021) 149447.

https://doi.org/https://doi.org/10.1016/j.scitotenv.2021.149447.

[16] S. Li, F. Ding, M. Flury, J. Wang, Dynamics of macroplastics and microplastics formed by biodegradable mulch film in an agricultural field, Sci. Total Environ. 894 (2023) 164674. https://doi.org/https://doi.org/10.1016/j.scitotenv.2023.164674.

[17] R. Bai, W. Wang, J. Cui, Y. Wang, Q. Liu, Q. Liu, C. Yan, M. Zhou, W. He, Modeling the temporal evolution of plastic film microplastics in soil using a backpropagation neural network, J. Hazard. Mater. 480 (2024) 136312. https://doi.org/https://doi.org/10.1016/j.jhazmat.2024.136312.

[18] K. Wang, W. Min, M. Flury, A. Gunina, J. Lv, Q. Li, R. Jiang, Impact of long-term conventional and biodegradable film mulching on microplastic abundance, soil structure and organic carbon in a cotton field, Environ. Pollut. 356 (2024) 124367. https://doi.org/https://doi.org/10.1016/j.envpol.2024.124367.

[19] X. Zhang, Y. Li, D. Ouyang, J. Lei, Q. Tan, L. Xie, Z. Li, T. Liu, Y. Xiao, T.H. Farooq, X. Wu, L. Chen, W. Yan, Systematical review of interactions between microplastics and microorganisms in the soil environment, J. Hazard. Mater. 418 (2021) 126288. https://doi.org/https://doi.org/10.1016/j.jhazmat.2021.126288.

[20] C. Li, Q. Cui, Y. Li, K. Zhang, X. Lu, Y. Zhang, Effect of LDPE and biodegradable PBAT primary microplastics on bacterial community after four months of soil incubation, J. Hazard. Mater. 429 (2022) 128353. https://doi.org/https://doi.org/10.1016/j.jhazmat.2022.128353.

[21] S. Lu, S. Wei, M. Li, D.R. Chadwick, M. Xie, D. Wu, D.L. Jones, Earthworms alleviate microplastics stress on soil microbial and protist communities, Sci. Total Environ. 948 (2024) 174945. https://doi.org/https://doi.org/10.1016/j.scitotenv.2024.174945.

[22] C. Accinelli, H.K. Abbas, V. Bruno, L. Nissen, A. Vicari, N. Bellaloui, N.S. Little, W. Thomas Shier, Persistence in soil of microplastic films from ultra-thin compostable plastic bags and implications on soil Aspergillus flavus

population, Waste Manag. 113 (2020) 312–318. https://doi.org/https://doi.org/10.1016/j.wasman.2020.06.011.

[23] M. Kamiya, S. Asakawa, M. Kimura, Molecular analysis of fungal communities of biodegradable plastics in two Japanese soils, Soil Sci. Plant Nutr. 53 (2007) 568–574. https://doi.org/10.1111/j.1747-0765.2007.00169.x.

[24] J. Zhang, D. Gao, Q. Li, Y. Zhao, L. Li, H. Lin, Q. Bi, Y. Zhao, Biodegradation of polyethylene microplastic particles by the fungus Aspergillus flavus from the guts of wax moth Galleria mellonella, Sci. Total Environ. 704 (2020) 135931. https://doi.org/https://doi.org/10.1016/j.scitotenv.2019.135931.

[25] P.-Y. Wang, Z.-Y. Zhao, X.-B. Xiong, N. Wang, R. Zhou, Z.-M. Zhang, F. Ding, M. Hao, S. Wang, Y. Ma, A.G. Uzamurera, K.-W. Xiao, A. Khan, X.-P. Tao, W.-Y. Wang, H.-Y. Tao, Y.-C. Xiong, Microplastics affect soil bacterial community assembly more by their shapes rather than the concentrations, Water Res. 245 (2023) 120581. https://doi.org/https://doi.org/10.1016/j.watres.2023.120581.

[26] A. Jakobs, E. Gürkal, J.N. Möller, M.G.J. Löder, C. Laforsch, T. Lueders, A novel approach to extract, purify, and fractionate microplastics from environmental matrices by isopycnic ultracentrifugation, Sci. Total Environ. 857 (2023) 159610. https://doi.org/https://doi.org/10.1016/j.scitotenv.2022.159610.

[27] B. Hufnagl, M. Stibi, H. Martirosyan, U. Wilczek, J.N. Möller, M.G.J. Löder, C. Laforsch, H. Lohninger, Computer-Assisted Analysis of Microplastics in Environmental Samples Based on μFTIR Imaging in Combination with Machine Learning, Environ. Sci. \& Technol. Lett. 9 (2022) 90–95. https://doi.org/10.1021/acs.estlett.1c00851.

[28] M. Kooi, A.A. Koelmans, Simplifying Microplastic via Continuous Probability Distributions for Size, Shape, and Density, Environ. Sci. \& Technol. Lett. 6 (2019) 551–557. https://doi.org/10.1021/acs.estlett.9b00379.

[29] A. Philippe, C. Noël, B. Eyheraguibel, J.-F. Briand, I. Paul-Pont, J.-F.

Ghiglione, E. Coton, G. Burgaud, Fungal Diversity and Dynamics during Long-Term Immersion of Conventional and Biodegradable Plastics in the Marine Environment, Diversity. 15 (2023). https://doi.org/10.3390/d15040579.

[30] M. Srikanth, T.S.R.S. Sandeep, K. Sucharitha, S. Godi, Biodegradation of plastic polymers by fungi: a brief review, Bioresour. Bioprocess. 9 (2022) 42. https://doi.org/10.1186/s40643-022-00532-4.

[31] B.W. Stone, J. Li, B.J. Koch, S.J. Blazewicz, P. Dijkstra, M. Hayer, K.S. Hofmockel, X.-J.A. Liu, R.L. Mau, E.M. Morrissey, J. Pett-Ridge, E. Schwartz, B.A. Hungate, Nutrients cause consolidation of soil carbon flux to small proportion of bacterial community, Nat. Commun. 12 (2021) 3381. https://doi.org/10.1038/s41467-021-23676-x.

[32] A. kanwal, M. Zhang, F. Sharaf, L. Chengtao, Screening and characterization of novel lipase producing Bacillus species from agricultural soil with high hydrolytic activity against PBAT poly (butylene adipate co terephthalate) co-polyesters, Polym. Bull. 79 (2022) 10053–10076. https://doi.org/10.1007/s00289-021-03992-4.

[33] Q. Huang, S. Kimura, T. Iwata, Thermal Embedding of Humicola insolens Cutinase: A Strategy for Improving Polyester Biodegradation in Seawater, Biomacromolecules. 24 (2023) 5836–5846. https://doi.org/10.1021/acs.biomac.3c00835.

[34] M. Giyahchi, H. Moghimi, The Role and Application of Microbial Enzymes in Microplastics' Bioremediation: Available and Future Perspectives, in: Bioremediation Removing Microplastics from Soil, n.d.: pp. 33–56. https://doi.org/10.1021/bk-2023-1459.ch003.

[35] C. Xu, S. Lu, Y. Cidan, H. Wang, G. Sun, M.U. Saleem, F.S. Ataya, Y. Zhu, Wangdui-Basang, K. Li, Microbiome analysis reveals alteration in water microbial communities due to livestock activities, Environ. Sci. Pollut. Res. 31 (2024) 47298–47314. https://doi.org/10.1007/s11356-024-34334-2.

[36] W. Guo, Z. Ye, Y. Zhao, Q. Lu, B. Shen, X. Zhang, W. Zhang, S.-C. Chen, Y. Li, Effects of different microplastic types on soil physicochemical properties,

enzyme activities, and bacterial communities, Ecotoxicol. Environ. Saf. 286 (2024) 117219. https://doi.org/https://doi.org/10.1016/j.ecoenv.2024.117219.

[37] K. Meng, P. Harkes, E. Huerta Lwanga, V. Geissen, Microplastics exert minor influence on bacterial community succession during the aging of earthworm (Lumbricus terrestris) casts, Soil Biol. Biochem. 195 (2024) 109480. https://doi.org/https://doi.org/10.1016/j.soilbio.2024.109480.

[38] L.H. Orellana, T. Ben Francis, M. Ferraro, J.-H. Hehemann, B.M. Fuchs, R.I. Amann, Verrucomicrobiota are specialist consumers of sulfated methyl pentoses during diatom blooms, ISME J. 16 (2022) 630–641. https://doi.org/10.1038/s41396-021-01105-7.

[39] L. Lu, Y. Han, Z. Liu, J. Qian, Y. Yan, Y. Sun, Effects of two new biodegradable films on tomato growth and soil microbial and enzyme activities., Shandong Agric. Sci. 55 (2023) 101–106. https://doi.org/10.14083/j.issn.1001-4942.2023.05.015.

[40] L.A. Hug, C.J. Castelle, K.C. Wrighton, B.C. Thomas, I. Sharon, K.R. Frischkorn, K.H. Williams, S.G. Tringe, J.F. Banfield, Community genomic analyses constrain the distribution of metabolic traits across the Chloroflexi phylum and indicate roles in sediment carbon cycling, Microbiome. 1 (2013) 22. https://doi.org/10.1186/2049-2618-1-22.

[41] Y. Sun, C. Duan, N. Cao, X. Li, X. Li, Y. Chen, Y. Huang, J. Wang, Effects of microplastics on soil microbiome: The impacts of polymer type, shape, and concentration, Sci. Total Environ. 806 (2022) 150516. https://doi.org/https://doi.org/10.1016/j.scitotenv.2021.150516.

[42] A.M. Breister, M.A. Imam, Z. Zhou, M.A. Ahsan, J.C. Noveron, K. Anantharaman, P. Prabhakar, Soil microbiomes mediate degradation of vinyl ester-based polymer composites, Commun. Mater. 1 (2020) 101. https://doi.org/10.1038/s43246-020-00102-1.

[43] W. Lin, Y. Zhao, T. Su, Z. Wang, Enzymatic hydrolysis of poly(butylene adipate-co-terephthalate) by Fusarium solani cutinase, Polym. Degrad. Stab. 211 (2023) 110335.

https://doi.org/https://doi.org/10.1016/j.polymdegradstab.2023.110335.